Biology of Reproduction, 2019, 100(2), 547–560
doi:10.1093/biolre/ioy200
Research Article
Advance Access Publication Date: 21 September 2018

Research Article

Sources of *all-trans* retinal oxidation independent of the aldehyde dehydrogenase 1A isozymes exist in the postnatal testis†

My-Thanh Beedle [1], Faith Stevison [2], Guo Zhong [2], Traci Topping [1], Cathryn Hogarth[1], Nina Isoherranen[2] and Michael D. Griswold[1,*]

[1]School of Molecular Biosciences and Center for Reproductive Biology, Washington State University, Pullman, Washington, USA and [2]Department of Pharmaceutics, University of Washington, Seattle, Washington, USA

*__Correspondence:__ School of Molecular Biosciences, Washington State University, PO Box 647520, Pullman, WA 99164, USA. E-mail: mgriswold@vetmed.wsu.edu

†__Grant support:__ This research was supported by U.S. National Institutes of Health grants RO1 10808 to MDG and U54 HD 42454 to MDG.

__Conference presentation:__ Presented in part at the 50th Annual Meeting of the Society for the Study of Reproduction, 13–16 July 2017, Washington D.C., USA.

Received 23 May 2018; Revised 1 August 2018; Accepted 11 September 2018

Abstract

Despite the essential role of the active metabolite of vitamin A, *all-trans* retinoic acid (*at*RA) in spermatogenesis, the enzymes, and cellular populations responsible for its synthesis in the postnatal testis remain largely unknown. The aldehyde dehydrogenase 1A (ALDH1A) family of enzymes residing within Sertoli cells is responsible for the synthesis of *at*RA, driving the first round of spermatogenesis. Those studies also revealed that the *at*RA required to drive subsequent rounds of spermatogenesis is possibly derived from the ALDH1A enzymes residing within the meiotic and post-meiotic germ cells. Three ALDH1A isozymes (ALDH1A1, ALDH1A2, and ALDH1A3) are present in the testis. Although, ALDH1A1 is expressed in adult Sertoli cells and is suggested to contribute to the *at*RA required for the pre-meiotic transitions, ALDH1A2 is proposed to be the essential isomer involved in testicular *at*RA biosynthesis. In this report, we first examine the requirement for ALDH1A2 via the generation and analysis of a conditional *Aldh1a2* germ cell knockout and a tamoxifen-induced *Aldh1a2* knockout model. We then utilized the pan-ALDH1A inhibitor (WIN 18446) to test the collective contribution of the ALDH1A enzymes to *at*RA biosynthesis following the first round of spermatogenesis. Collectively, our data provide the first in vivo evidence demonstrating that animals severely deficient in ALDH1A2 postnatally proceed normally through spermatogenesis. Our studies with a pan-ALDH1A inhibitor (WIN 18446) also suggest that an alternative source of *at*RA biosynthesis independent of the ALDH1A enzymes becomes available to maintain *at*RA levels for several spermatogenic cycles following an initial *at*RA injection.

Summary Sentence

Elimination of ALDH1A enzymatic activity following a single pulse of retinoic acid does not immediately ablate spermatogenesis due to the presence of an additional source of *at*Retinal oxidation.

Key words: spermatogenesis, Aldh1A, Aldh1a2, WIN 18,446, testis, spermatogonia, retinoic acid.

Introduction

Spermatogenesis is the process whereby spermatogonia proliferate and differentiate to generate the male reproductive gametes, spermatozoa [1–4]. The transition of A undifferentiated spermatogonia into A1 differentiating spermatogonia (A to A1 transition, or spermatogonial differentiation) is a critical regulatory step during spermatogenesis [1–4]. The A to A1 transition occurs at periodic intervals of 8.6 days along the length of testis tubules, resulting in the appearance of 12 reoccurring sets of cellular associations called stages [5–7]. The stepwise appearance of each of these stages ensures the asynchronous nature of the spermatogenetic wave and maintains the continuous release of sperm [5, 6]. Extensive evidence exists demonstrating that *all-trans* retinoic acid (*at*RA) is absolutely required for the initiation and maintenance of the spermatogenic wave [8]. While the necessity of *at*RA for spermatogenesis has been widely validated, the cellular source and the enzymatic families responsible for its synthesis in the postnatal testis are not completely understood.

A role for *at*RA, the active derivative of vitamin A, in spermatogenesis was initially identified in rodents fed a vitamin A-deficient (VAD) diet [9]. Histological analysis of VAD testes revealed an arrest at the A to A1 transition that was readily reversed by an exogenous *at*RA injection. Surprisingly, spermatogenesis was restored in a synchronous manner, resulting in the pulsatile release of sperm [10–12]. Although a thorough understanding of the retinoid metabolizing enzymes are still being shaped in the mammalian testis, the currently accepted model for the conversion of vitamin A to *at*RA involves a two-step enzymatic pathway. The first step involves the oxidation of *all-trans* retinol (*at*ROL) to *all-trans* retinaldehyde (*at*RAL) by the cytosolic alcohol dehydrogenases or the microsomal retinol dehydrogenases [13–19]. This step is generally considered to be reversible and rate limiting. In contrast, the second reaction is irreversible and involves the conversion of *at*RAL to *at*RA by the aldehyde dehydrogenase 1A (ALDH1A) family [20–22]. The ALDH1A family of enzymes includes three isozymes that have roles in *at*RA synthesis: ALDH1A1 [23], ALDH1A2 [24], and ALDH1A3 [13, 25–27]. Localization studies have shown that the ALDH1A isoforms exhibit cell-specific expression patterns within the testis, suggestive of distinct biological functions [28–30]. Specifically, *Aldh1a1* transcripts were detected in Leydig cells, and transcripts for *Aldh1a2* were detected in spermatogonia, spermatocytes, and spermatids [31–36]. Transcripts for *Aldh1a1* and *Aldh1a2* were also detected in prepubertal and adult Sertoli cells [31, 32]. ALDH1A3 was detected at very low levels in Leydig cells, spermatocytes, and spermatids within the 30 dpp testis [35, 37, 38]. Studies with a pan-ALDH1A inhibitor, WIN 18446 (WIN), revealed that the ALDH1A enzymes are collectively responsible for more than 95% of *at*RA biosynthesis in the wild-type mouse testis, with ALDH1A2 estimated to contribute to over 61% [23, 39–43]. Inhibition of the ALDH1A enzymes in neonatal mice via treatment with WIN followed by an *at*RA injection results in testes that are enriched for germ cells synchronously proceeding through development [44]. The strong inhibitory effects of WIN on the ALDH1A enzymes makes this chemical treatment a powerful tool to address questions regarding the contributions of the ALDH1A enzymes to retinoid-dependent processes such as spermatogenesis.

Accumulating evidence suggests that the sources of the *at*RA signal are differentially regulated between the first round and subsequent rounds of spermatogenesis. Specifically, it has been shown that the *at*RA required to drive the first round of spermatogenesis is derived from the ALDH1A enzymes residing within Sertoli cells [31]. The enzymatic and cellular sources of *at*RA biosynthesis driving the subsequent rounds of spermatogonial differentiation remain to be identified; however, it is widely hypothesized that the ALDH1A enzymes, specifically ALDH1A2, residing within the meiotic and postmeiotic germ cells are involved [31, 32, 38, 45]. The in vivo role that *Aldh1a2* plays within germ cells has yet to be determined, as global *Aldh1a2*-null mice die early in embryonic development (E9.5–10.5) [39, 40, 46]. To overcome the embryonic lethality associated with the null model, we utilized traditional Cre-lox technology to generate animals in which *Aldh1a2* was excised postnatally beginning in the differentiating germ cells (via the *Stra8*-Cre) and globally (via the tamoxifen-inducible Cre). To our knowledge, these genetic models are the first in vivo demonstration that severe deficiency of ALDH1A2 within the postnatal testis does not negatively affect spermatogenic progression. To address the collective contribution of the three major ALDH1A isozymes to testicular *at*RA biosynthesis, we also utilized the pan-ALDH1A inhibitor, WIN 18446. Surprisingly, potent inhibition of the ALDH1A enzymes (via WIN 18446 treatment) was not sufficient to immediately block subsequent rounds of spermatogonial differentiation, nor did it result in significantly reduced *at*RA levels. Additional in vivo studies simultaneously using WIN 18446 and hydralazine (HYD), a potent inhibitor of the aldehyde oxidases (AOXs) (another family of enzymes capable of catalyzing the *at*RAL to *at*RA oxidation reaction), suggested that the AOX family of enzymes may play a previously unexplored role in testicular *at*RA biosynthesis. Collectively, our studies suggest that multiple enzyme families may be capable of synthesizing *at*RA in the postnatal testis driving the second and subsequent rounds of spermatogenesis.

Materials and methods

Animal care and ethics statement

All animal care and procedures were conducted according to protocols and guidelines approved by the Washington State University Committee on the Use and Care of Animals. Studies were performed with male mice that were housed in a humidity- and temperature-controlled room with access to water and food ad libitum. Mice were euthanized by CO_2 asphyxiation followed by cervical dislocation.

Mouse lines, mouse breeding, and PCR genotype analysis

The *Aldh1a2*$^{fl/fl}$ transgenic line was generated by the Mouse Biology Program (MBP) at the University of California, Davis. The targeting construct and the replacement vector strategy used to generate the *Aldh1a2*$^{fl/fl}$ transgenic line is provided in Supplemental Figure S1 and details regarding the generation of the line can also be found in Supplemental Methods (Supplemental Data are available online at www.biolreprod.org). *Aldh1a2*$^{fl/fl}$ females were mated with *Aldh1a2*$^{fl/+}$, *Stra8*-Cre [47] male mice to generate *Aldh1a2*$^{fl/fl}$, *Stra8*-Cre negative (control) and *Aldh1a2*$^{fl/fl}$, *Stra8*-Cre positive (cKO) animals. The *Stra8*-Cre (Stock number #008208) line was purchased from the Jackson Laboratory (Bar Harbor, ME). To generate the tamoxifen-inducible global knockout of *Aldh1a2*, we utilized the B6.129-Gt(Rosa)26Sor$^{tm1(cre/ERT2)Tyj}$ (Stock number #008463, hereafter referred to as CreER^{T2}) transgenic line, purchased from the Jackson Laboratory (Bar Harbor). Administration of tamoxifen (via intraperitoneal injection) induces the CreER^{T2} fusion protein to

translocate to the nucleus and excise floxed DNA fragments. For simplicity, mice whose floxed allele was excised following tamoxifen injection will hereafter be denoted by *Aldh1a2*$^{\Delta}$. Adult *Aldh1a2*$^{fl/fl}$ female mice were crossed with *Aldh1a2*$^{+/+}$, CreER^{T2} homozygous males to generate F1 animals heterozygous for both genes. These heterozygous animals were mated together to generate F2 animals. F2 animals that were heterozygous for *Aldh1a2* (*Aldh1a2*$^{fl/+}$) and homozygous for the CreER^{T2} were mated to generate F3 experimental animals. This breeding scheme generated animals with the following genotypes within the F3 generation: *Aldh1a2*$^{+/+}$, CreER^{T2}; *Aldh1a2*$^{fl/+}$, CreER^{T2}; and *Aldh1a2*$^{fl/fl}$, CreER^{T2}. To determine the genotypes of experimental mice, genomic DNA samples were extracted from a small piece of tail or ear tissue, which served as templates for PCR reactions. Allele-specific PCR reactions were performed using primer sets described in Supplemental Table S1. PCR detection of the excised allele was performed on all experimental mice before (obtained from tail clip) and after (obtained from ear/tail chip) tamoxifen injection. Prior to the tamoxifen injection, the excised band was never detected in any genomic samples regardless of the animal's genotype. No excision bands were detected in any of the *Aldh1a2*$^{+/+}$, CreER^{T2} animals injected with tamoxifen. However, a prominent excision band was detected in all *Aldh1a2*$^{\Delta/+}$, CreER^{T2} and *Aldh1a2*$^{\Delta/\Delta}$, CreER^{T2} animals.

Tamoxifen preparation and administration

Tamoxifen (Tm, Sigma T5648) was dissolved in 10% ethanol and 90% sesame oil at a concentration of 20 mg/ml, which was subsequently wrapped in foil to protect the solution from light. *Aldh1a2*$^{+/+}$, CreER^{T2}; *Aldh1a2*$^{fl/+}$, CreER^{T2}; and *Aldh1a2*$^{fl/fl}$, CreER^{T2} animals aged 8 or 21 dpp were administered 80 mg/kg tamoxifen via an intraperitoneal injection for either three or five consecutive days, respectively [48]. For all injection strategies, animals were left to recover for 60 additional days prior to analysis.

Fertility evaluation

Adult *Aldh1a2*$^{fl/fl}$, *Stra8*-Cre control and cKO males (n = 4 per genotype) were housed with 129/B6 wild-type adult females of known fertility at a male-to-female sex ratio of 1:2. Males were observed for normal mounting behavior and female mice were checked each morning for the presence of a copulatory plug. The sex of the offspring, the total number of offspring, and the number of litters produced over a 4-month fertility trial were recorded.

RNA isolation and quantitative real-time polymerase chain reaction

Testis samples for quantitative real-time polymerase chain reaction (qRT-PCR) analysis were snap-frozen on dry ice upon removal and stored at –80°C. Tissues were homogenized and total RNA was extracted using TRIzol reagent (15596018, Ambio Life Technologies) according to the manufacturer's directions. RNA quality and quantity was determined using a NanoDrop 1000 Spectrophotometer (Thermo Scientific). Total RNA (250–500 ng) was reverse-transcribed using the iScript cDNA synthesis kit (1708891, Bio-Rad). Quantitative RT-PCR was performed using Fast SYBR Green PCR Mastermix (4385612, Applied Biosystems) on a 7500 Fast PCR System (Applied Biosystems). Primer sequences for the genes analyzed are presented in Supplemental Table S2. The expression of these genes was determined from three to six mice, each of which was measured in triplicate and averaged. The relative mRNA levels in each sample were calculated using the comparative CT method ($\Delta\Delta C_T$) [49]. The values were normalized using the expression of the ribosomal protein S2 (*Rps2*).

WIN, hydralazine treatments, and atRA injections

We utilized a previously published WIN7D + RA synchrony protocol with minor modifications [44, 45]. Briefly, 2 dpp 129/B6 male mice were pipette fed 100 mg/kg/bw (body weight) WIN (gift from Dr John Amory) daily for 7 days, given an *at*RA injection on day 9 and maintained on one of the following treatment regimens during the injection recovery: (1) 1% gum tragacanth (WIN7D + RA), (2) 150 mg/kg/bw WIN (WIN7D + RA + WIN), (3) 25 mg/kg/bw of HYD (Sigma-Aldrich, H1753) (WIN7D + RA + HYD), or (4) 150 mg/kg/bw WIN and 25 mg/kg/bw HYD (WIN7D + RA + WIN/HYD) (Supplemental Figure S2). Depending on the experiment, the lengths of the WIN maintenance treatments were 8, 16, 24, 32, or 40 days. A group of animals were fed 100 mg/kg/bw WIN from 2–8 dpp, injected with vehicle control (dimethylsulfoxide, DMSO) injection on day 9, and then maintained on 150 mg/kg/bw WIN during injection recovery (WIN7D + DMSO + WIN; Supplemental Figure S2). An additional group of animals were pipette fed 1% gum tragacanth for the duration of the treatment regimen (Supplemental Figure S2). Mice given *at*RA injections were subcutaneously injected with 200 μg *at*RA (Sigma-Aldrich, R2625) suspended in 10 μl DMSO (Fisher Scientific, BP231-1). The WIN compound was suspended in 1% gum tragacanth and HYD was suspended in ddH_2O. Irrespective of the type of injection that the animals received (*at*RA or DMSO), WIN or HYD-maintained animals also received WIN or HYD on the day of the injection.

Immunohistochemistry

Immunohistochemistry (IHC) was performed as previously described [50] with the exception that the primary antibodies used were aldehyde dehydrogenase family 1 member A2 (ALDH1A2; 1:100 dilution; 13951-1-AP; Proteintech Group), stimulated by retinoic acid 8 (STRA8; antibody produced in-house) [51], zinc finger and BTB domain containing 16 (ZBTB16; 1:500 dilution; sc-22839; Santa Cruz Biotechnology), germ cell nuclear antigen (GCNA; gift from Dr. George Enders), and SRY (sex dertermining region Y) - box 9 (SOX9; 1:500 dilution; AB5535; EMD Millipore). Control sections were incubated in blocking solution with the primary antibody omitted.

Measurement of testicular atRA levels

For testicular *at*RA measurement of the *Aldh1a2*, *Stra8*-Cre and *Aldh1a2*, CreER^{T2} animals (n = 3–4 per treatment), testis tissue (30–50 mg) was homogenized in 5X tissue-weight saline. Tissue homogenates (120 μL) were transferred into 1.7 ml Eppendorf tubes followed by the addition of 5 μL of 2 μM *at*-RA-d_5 as an internal standard. Acetonitrile (240 μL) was added to tissue homogenates to precipitate proteins. After 5–10 s of vortexing, samples were left on ice for 10 min and then centrifuged at 18 000 × g at 4°C for 30 min. Supernatant was transferred to glass vials for liquid chromatography-tandem mass spectrometry (LC-MS/MS) analysis as described in published methods [36, 52]

For testicular *at*RA measurement of WIN treated mice, each data point (n = 3–4 per treatment group) was obtained from pooled testes of 8–15 treated mice (188–226 mg per sample). The extraction pro-

tocol and LC-MS/MS method used to measure WIN-treated animals were performed as described in references [36, 51–53].

Cell quantification

Serial sections for cell quantifications were separated by a minimum of 20 μm. Immunostaining of testis sections for ZBTB16, STRA8, GCNA, or SOX9 was performed as described above. The different cell types were identified based on (1) ZBTB16-, STRA8-, GCNA-, or SOX9-positive immunostaining; (2) the shape and size of the nuclei; and (3) the location of the cells within the seminiferous tubules. Quantification was performed to count (1) the number of ZBTB16-, STRA8-, or SOX9-immunopositive spermatogonia, or (2) the number of tubules displaying normal versus absent/missing layers of GCNA-positive germ cells within 200 tubules per animal. All quantification was performed using a minimum of three animals per treatment group for each experiment.

Statistical analysis

Statistical significance between two experimental groups was evaluated using the Student *t*-test (Prism; Version 7.0c; Graphpad), while statistical significance between more than two groups was determined using a one-way ANOVA (Tukey's HSD post hoc test; Prism; Version 7.0c; Graphpad). A *P*-value of 0.05 or less was considered statistically significant, and all data are presented as mean ± standard error of the mean (SEM).

Results

Germ cell-specific deletion of Aldh1a2 does not result in abnormal histological phenotypes

To explore the role of *Aldh1a2* specifically in postnatal germ cells, we generated an animal with a germ cell-specific deletion of *Aldh1a2* using the *Stra8*-Cre. The *Stra8*-Cre was chosen because it is expressed around 3 dpp in a select population of A_{al} spermatogonia and in all A_1 differentiating spermatogonia [47]. Expression of the Cre protein should eliminate *Aldh1a2* within the germ cell populations of interest (namely the preleptotene spermatocytes, pachytene spermatocytes, and spermatid populations). *Aldh1a2* control and cKO animals were obtained at the expected Mendelian frequencies, and cKO mice were morphologically indistinguishable from their control littermates. To verify that we had generated a genuine germ cell-specific *Aldh1a2* cKO, we used a previously characterized antibody against ALDH1A2 to localize the protein on testis sections of control and cKO mice at 60 and 180 dpp by IHC [37]. Consistent with published results, we observed abundant ALDH1A2-positive spermatogonia, spermatocytes, spermatids, and Leydig cells in all control testis sections (Figure 1A and Supplemental Figure S3A and B; n = 4). The ALDH1A2 protein was undetectable within the seminiferous epithelium of cKO mice; however, we detected ALDH1A2-positive cells within the interstitial space (Figure 1B and Supplemental Figure S3C and D; n = 4). Quantitative RT-PCR analysis also demonstrated that *Aldh1a2* expression was significantly reduced in cKO animals at 60 and 180 dpp compared to controls (Figure 1C and Supplemental Figure S3E; n = 3–6). To determine whether *Aldh1a1* and *Aldh1a3* are upregulated in response to reduced levels of *Aldh1a2*, we performed qRT-PCR in 60 and 180 dpp testes from cKO mice and found no statistically significant changes in the expression of *Aldh1a1* or *Aldh1a3* between the cKO and control testes at either age point (Figure 1C and Supplemental Figure S3E; n = 3–6).

Elimination of Aldh1a2 via Stra8-Cre does not significantly reduce atRA levels

To get an indirect measure of the *at*RA levels in the *Aldh1a2* cKO testes, we performed qRT-PCR for the expression of *at*RA target genes *Stra8* (stimulated by retinoic acid 8) and *Cyp26a1* (cytochrome P450 family 26 subfamily A member 1) [54]. A significant reduction in the expression of *Stra8* was observed in the 180 dpp testis (Figure 1C; n = 4). We also detected a significant reduction in the expression of *Cyp26a1* in the 60 and 180 dpp testes (Figure 1C and Supplemental Figure S3E; n = 4). As *Cyp26a1* has been used as an indirect indicator of tissue retinoid levels [55], these gene expression differences prompted us to quantify the *at*RA levels within these testes via LC-MS/MS. No significant reduction in the levels of *at*RA was measured in the 60 or 180 dpp cKO animals compared to the age-matched controls (Figure 1D and Supplemental Figure S3F; n = 3–4).

Elimination of Aldh1a2 within germ cells does not alter the reproductive capacity of cKO mice

To determine whether elimination of *Aldh1a2* within the germ cells resulted in any adverse effects on the reproductive capacity of cKO mice, *Aldh1a2* control (n = 4) and cKO (n = 4) male mice (approximately 60 days old) were paired with two wild-type female mice each of known fertility for a 4-month fertility study. All males, regardless of genotype, displayed normal breeding behavior (i.e. normal mounting behavior and copulatory plug production). Female mice (n = 8) mated with *Aldh1a2*, *Stra8*-Cre control males produced an average of 5.25 litters, with an average of 6.7 ± 0.4 pups per litter (Supplemental Table S3). Female mice (n = 8) mated with *Aldh1a2*, *Stra8*-Cre cKO males produced an average of 5 litters, with an average of 6.6 ± 0.3 pups per litter (Supplemental Table S3). The average number of pups sired per litter was not significantly different between the control and cKO males (Figure 1E).

Tamoxifen-inducible postnatal global deletion of Aldh1a2 results in normal testicular histology and no significant reduction in atRA levels

Our IHC analysis of *Aldh1a2* cKO testes demonstrated ALDH1A2 expression within the interstitial space (Figure 1B and Supplemental Figure S3C and D; n = 4). As ALDH1A2 has been localized to Leydig cells and macrophages, we wanted to rule out the possibility that the activity of the ALDH1A2 enzymes within the interstitial space was sufficient to drive the qualitatively normal spermatogenesis observed in the *Aldh1a2* cKO [37, 56]. To accomplish this, we utilized the $CreER^{T2}$ transgenic line to generate animals in which global excision of the *Aldh1a2* allele can be induced by the administration of tamoxifen. No significant differences in the body weights of the tamoxifen-treated animals were observed on the day of euthanasia, regardless of their genotype or the age at which tamoxifen was administered (Supplemental Figure S4; n = 5–8). We used IHC to compare ALDH1A2 protein expression in testis cross sections from $Aldh1a2^{+/+}$, $CreER^{T2}$; $Aldh1a2^{\Delta/+}$, $CreER^{T2}$; and $Aldh1a2^{\Delta/\Delta}$, $CreER^{T2}$ animals injected with tamoxifen at 8 and 21 dpp (Figure 2A–F; n = 3–7). ALDH1A2 protein expression was robustly detected in the interstitial space, spermatocytes, and spermatids of the $Aldh1a2^{+/+}$, $CreER^{T2}$, and $Aldh1a2^{\Delta/+}$, $CreER^{T2}$ animals (Figure 2A, B, D and E; n = 3–7). In contrast, ALDH1A2 protein expression was not detected in the seminiferous epithelium of $Aldh1a2^{\Delta/\Delta}$, $CreER^{T2}$ animals; however, we were able to detect faint ALDH1A2 staining within the interstitial space (Figure 2C and

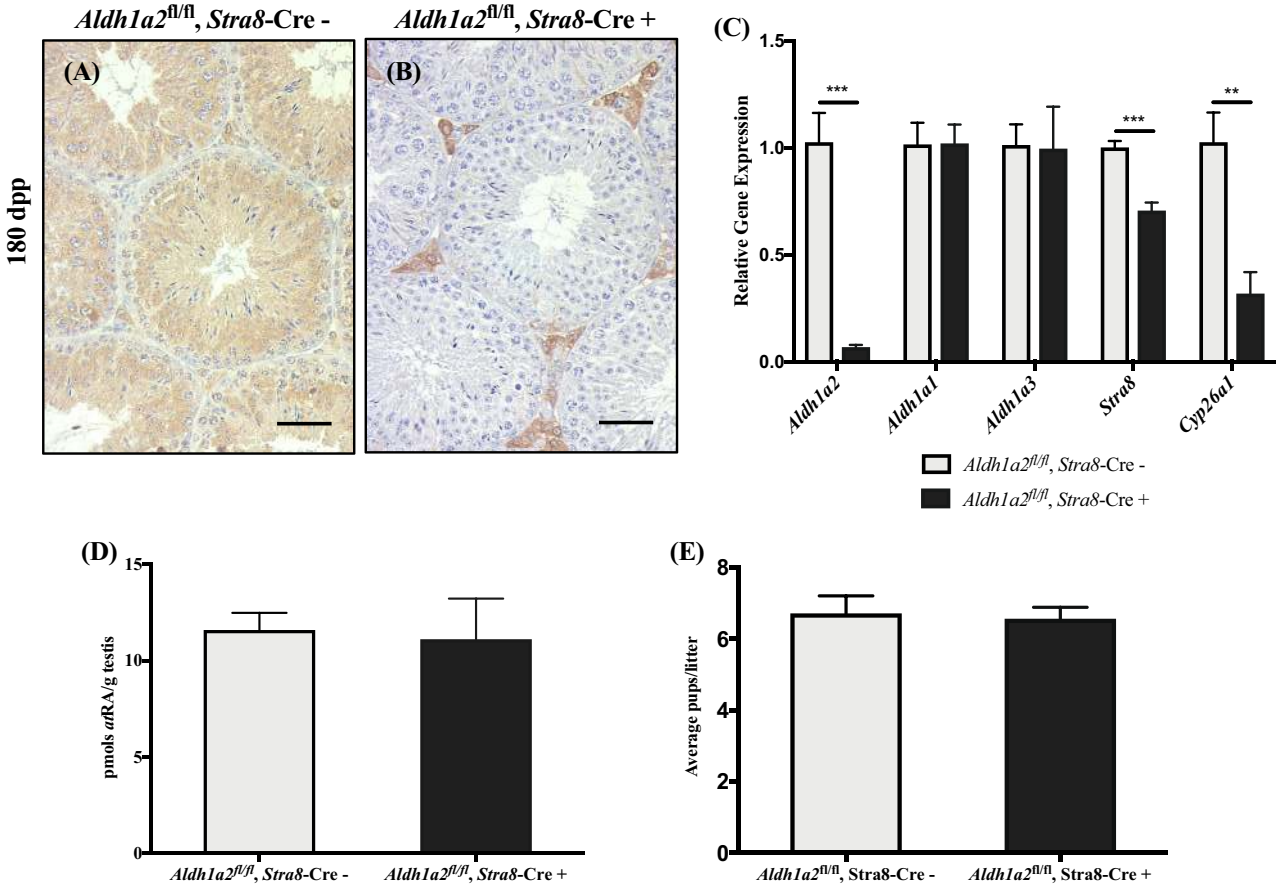

Figure 1. Elimination of *Aldh1a2* using the *Stra8*-Cre. Control (*Aldh1a2*$^{fl/fl}$, *Stra8*-Cre–) and cKO (*Aldh1a2*$^{fl/fl}$, *Stra8*-Cre+) animals analyzed at 180 dpp. Representative control (**A**) and cKO (**B**) cross-section stained for ALDH1A2. Immunopositive cells are indicated by brown precipitate. (**C**) qRT-PCR analysis of *Aldh1a2, Aldh1a1, Aldh1a3, Stra8,* and *Cyp26a1*. (**D**) Graphical representation of *at*RA measurements. **(E)** Graphical representation of the average number of pups per litter. Scale bars = 100 μM. n = 3–4. * $P < 0.05$, ** $P < 0.01$, and *** $P < 0.001$.

F; n = 3–7). We performed qRT-PCR to determine the degree of *Aldh1a2* reduction in the tamoxifen-treated testes. As anticipated, *Aldh1a2* transcript levels were decreased by approximately 50% in all *Aldh1a2*$^{\Delta/+}$, CreER^{T2} animals and 96–99% in all *Aldh1a2*$^{\Delta/\Delta}$, CreER^{T2} animals (Figure 2G and H; n = 4–5). No significant changes in the expression levels of *Aldh1a1* and *Aldh1a3* were measured by qRT-PCR (Figure 2G and H; n = 4–5). The expression of *Stra8* was not significantly different between the three genotypes in age-matched animals (Figure 2G and H; n = 4–5). However, expression of *Cyp26a1* was significantly reduced in the *Aldh1a2*$^{\Delta/\Delta}$, CreER^{T2} animals compared to *Aldh1a2*$^{+/+}$, CreER^{T2}, and *Aldh1a2*$^{\Delta/+}$ animals (Figure 2G and H; n = 4–5). No significant reduction in *at*RA levels was observed in the testes of mice injected with tamoxifen at 8 or 21 dpp as measured by LC-MS/MS (Figure 2I; n = 3–7).

Maintenance on WIN for one spermatogenic cycle following the WIN7D + RA synchrony protocol significantly increases the number of ZBTB16-positive spermatogonia but does not result in reduced *at*RA levels

To determine the contribution of all the ALDH1A enzymes to *at*RA biosynthesis, we utilized a WIN7D + RA synchrony protocol previously established in our laboratory [44]. This protocol involves the maintenance of 2 dpp mice on WIN 18446 for 7 days followed by an injection of *at*RA. WIN is a potent inhibitor of the ALDH enzymes, and treatment of neonatal mice with WIN for 7 consecutive days reduces *at*RA levels and results in testes that are enriched for undifferentiated spermatogonia [44]. An exogenous injection of *at*RA induces the arrested undifferentiated spermatogonia to simultaneously differentiate [44]. If the WIN treatment was continued for 1 cycle or 8 days following the injection of *at*RA (WIN7D + RA + WIN8D), we could address the contribution of the ALDH1A enzymes following the initial *at*RA pulse synthesized by the Sertoli cells during normal spermatogenesis. Additionally, this protocol generates testes that are synchronously undergoing spermatogenesis, eliminating the complexity associated with the heterogeneous nature of spermatogenesis in wild-type rodents. Our experimental design included four treatment groups: (1) unsynchronized animals, (2) animals given WIN7D + RA + 8D resulting in synchronized testes, (3) animals given WIN7D + RA + WIN8D (8 additional days of WIN 18446 treatment), and (4) animals given WIN7D + DMSO + WIN8D (continuous WIN 18446 treatment and no *at*RA) (Supplemental Figure S5A). The 8-day WIN maintenance protocol did not significantly alter the body weights of animals (Supplemental Figure S5B; n = 28–46). However, on the day of eu-

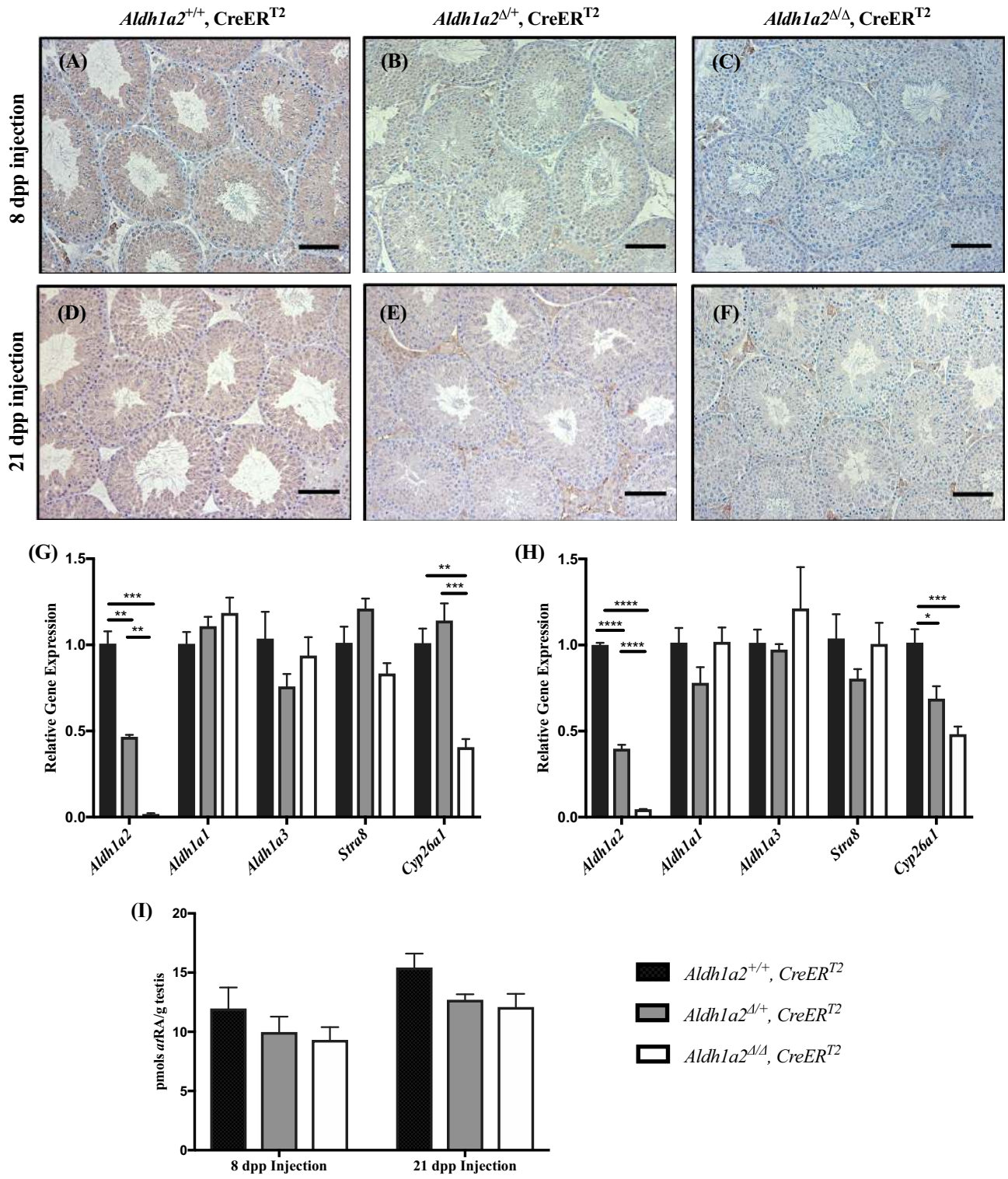

Figure 2. Elimination of *Aldh1a2* using the inducible CreER^{T2}. Analysis of *Aldh1a2*$^{+/+}$, CreER^{T2}; *Aldh1a2*$^{\Delta/+}$, CreER^{T2}; and *Aldh1a2*$^{\Delta/\Delta}$, CreER^{T2} animals injected with tamoxifen. Representative immunohistochemistry from animals injected at 8 (**A**, **B,** and **C**; 68 dpp at euthanasia) and 21 dpp (**D**, **E** and **F**; 81 dpp at euthanasia). Cross-sections are stained for ALDH1A2 protein and immunopositive cells are indicated by brown precipitate. qRT-PCR analysis was performed to determine the relative expression of *Aldh1a2, Aldh1a1, Aldh1a3, Stra8,* and *Cyp26a1* in animals injected with tamoxifen at 8 (**G**) and 21 dpp (**H**). (**I**) Graphical representation of *at*RA measurements. Scale bars = 100 μm. n = 3–7. $^{*}P < 0.05$, $^{**}P < 0.01$, $^{***}P < 0.001$, and $^{****}P < 0.0001$.

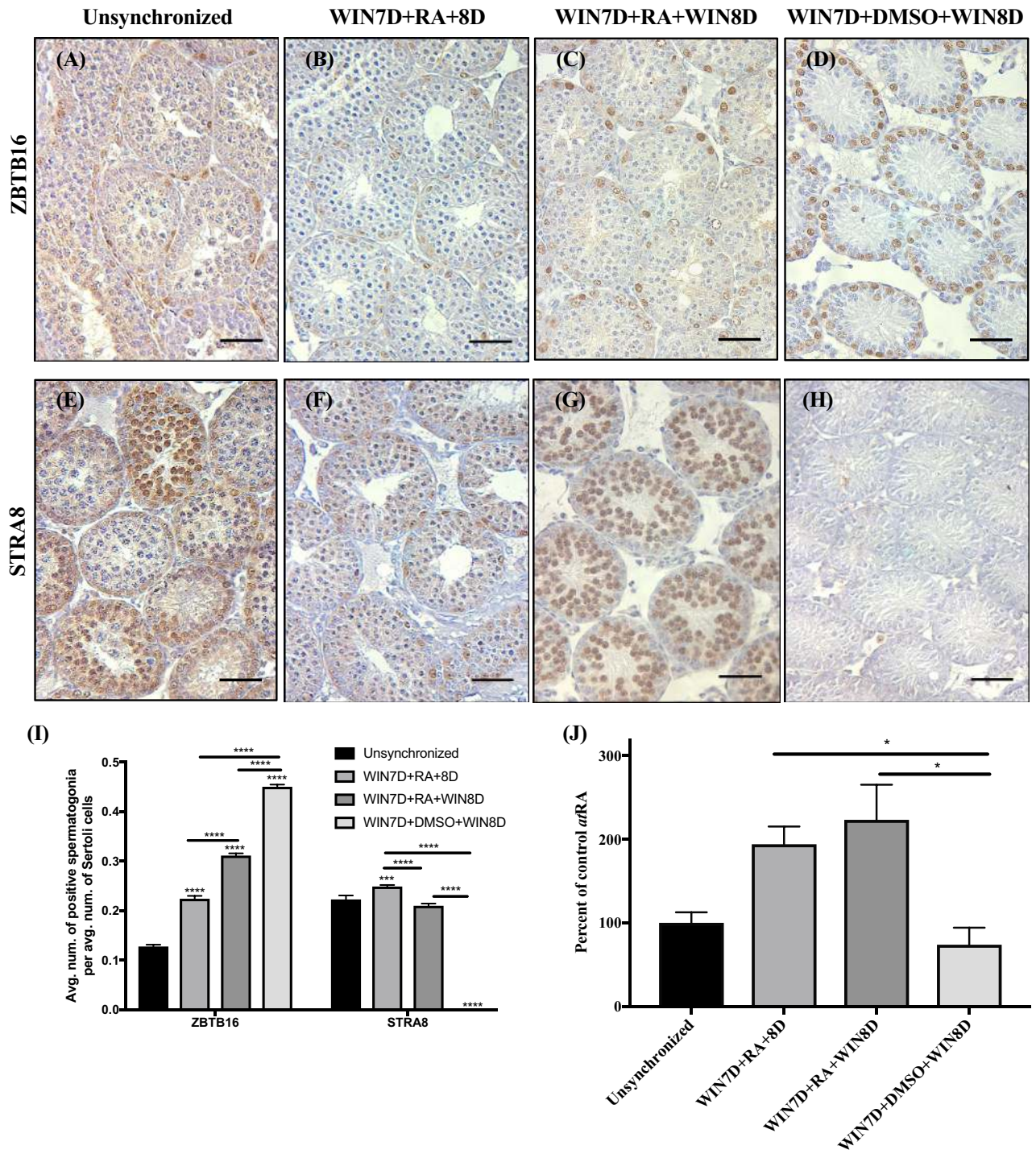

Figure 3. Maintenance on WIN7D + RA + WIN8D increases the number of ZBTB16-positive spermatogonia but does not decrease the number of STRA8-positive spermatogonia or *at*RA levels. Immunostaining of testis sections from unsynchronized (**A** and **E**), WIN7D + RA + 8D (**B** and **F**), WIN7D + RA + WIN8D (**C** and **G**), and WIN7D + DMSO + WIN8D treated mice (**D** and **H**). Testis sections were immunostained for ZBTB16 (**A**–**D**) and STRA8 (**E**–**H**) protein. For each treatment group, immmunopositive cells are denoted by brown precipitate. (**I**) Graphical representation of ZBTB16 and STRA8 counts. (**J**) Graphical representation of *at*RA measurements reported as percent of control. Asterisks represent statistical difference of a treatment group compared to control. Black lines represent statistical significance between treatment groups. Animals were 17 dpp at euthanasia. Scale bar = 100 μM. n = 3–4. $^{*}P < 0.05$, $^{***}P < 0.001$, $^{****}P < 0.0001$.

thanasia, the testis weights of unsynchronized, WIN7D + RA + 8D, and WIN7D + RA + WIN8D treated animals were significantly greater than those of the WIN7D + DMSO + WIN8D treated animals (Supplemental Figure S5C; n = 8–46). We hypothesized that if the ALDH1A family of enzymes is the major enzymatic family involved in *at*RA synthesis during subsequent rounds of spermatogenesis, then WIN7D + RA + WIN8D treated animals would display reduced spermatogonial differentiation compared to the unsynchronized and WIN7D + RA + 8D treated animals. To assess this, we first immunostained and quantified testis sections for the ZBTB16 protein that marks undifferentiated spermatogonia and SOX9 protein which marks Sertoli cells (Figure 3A–D; n = 3) [57, 58]. There was an average of 0.127 ± 0.003 ZBTB16-positive spermatogonia per average number of Sertoli cells in unsynchronized animals (Figure 3I; n = 3). WIN7D + RA + 8D, WIN7D + RA + WIN8D, and WIN7D + DMSO + WIN8D treated animals displayed a 1.8-, 2.4-, and 3.5-fold increase in the average number of ZBTB16-positive spermatogonia per average number of Sertoli cells, respectively, relative to the unsynchronized animals (Figure 3I; n = 3). We also immunostained testis sections for the STRA8 protein that marks differentiating spermatogonia and quantified the proportion of STRA8-positive spermatogonia per average number of Sertoli cells (Figure 3E–H and I; n = 3) [59]. STRA8 was expressed in a heterogeneous manner in testis sections obtained from the unsynchronized animals, whereas synchronous expression of STRA8 was detected in WIN7D + RA + 8D and WIN7D + RA + WIN8D treated animals (Figure 3E–G; n = 3). No detectable STRA8-positive differentiating spermatogonia were detected in the WIN7D + DMSO + WIN8D treated animals (Figure 3H; n = 3). The average number of STRA8-positive differentiating spermatogonia in the unsynchronized, WIN7D + RA + 8D, and WIN7D + RA + WIN8D treated groups were significantly increased compared to the WIN7D + DMSO + WIN8D treated animals (Figure 3I; n = 3). To determine whether the STRA8 counts were reflective of the *at*RA levels within treated testes, we measured *at*RA levels by LC-MS/MS. The amounts of *at*RA measured in the WIN7D + RA + 8D and WIN7D + RA + WIN8D treated groups were significantly greater than those measured for the WIN7D + DMSO + WIN8D treated animals (Figure 3J; n = 3–4).

Maintenance on WIN for several spermatogenic cycles following the WIN7D + RA synchrony protocol eventually results in degenerative seminiferous tubules

Since 1 cycle or 8 days of additional WIN treatment was unable to arrest spermatogonial differentiation following the *at*RA injection, we hypothesized that several additional cycles of treatment were required. To test this, we maintained several groups of animals on WIN for 16, 24, 32, or 40 additional days following the *at*RA or DMSO injections (Supplemental Figure S6). For comparison purposes, we also maintained unsynchronized and WIN7D + RA treated animals for 16, 24, 32, and 40 day recovery periods (Supplemental Figure S6). Histological analyses were performed to examine STRA8 expression (Figure 4; n = 3–4). Untreated, unsynchronized animals displayed a heterogeneous pattern of STRA8 expression within spermatogonia and preleptotene/leptotene spermatocytes as expected (Figure 4A, E, I, and N; n = 3–4). STRA8 expression was detected in spermatogonia and preleptotene spermatocytes in WIN7D + RA + 16D, WIN7D + RA + 24D, and WIN7D + RA + 40D treated animals but was rare in the WIN7D + RA + 32D treated animals (Figure 4B, F, J, and O; n = 3–4). A high degree of phenotypic heterogeneity was observed in the WIN7D + RA + WIN32D group, as some males displayed testis tubules with normal histology while others had a mixture of morphologically normal tubules adjacent to those with apoptotic cells and missing advanced germ cells (Figure 4 L and M; n = 4). In all WIN7D + RA + WIN40D animals, severe testis degeneration was observed (Figure 4Q; n = 4). No STRA8-positive spermatogonia were detected in any of the animals given a DMSO injection and maintained on WIN for 16, 24, 32, or 40 days (Figure 4C, G, K, and P; n = 3–4).

Maintenance on WIN and HYD for one spermatogenic cycle following the WIN7D + RA synchrony protocol increases the number of ZBTB16-positive spermatogonia

Although WIN is a potent pan-ALDH1A inhibitor, approximately 32–40 days of WIN maintenance was required for severe seminiferous tubule degeneration when administered after an *at*RA pulse. Based on these findings, we hypothesized that an alternative source of *at*RA synthesis, independent of the ALDH1A enzymes, becomes available following the *at*RA injection. Of the enzyme families capable of catalyzing the *at*RAL to *at*RA reaction, transcripts for members of the AOX family were identified in microarray sequencing experiments previously performed in our laboratory [60, 61]. To test their potential contribution to *at*RA biosynthesis, we maintained animals on a potent inhibitor of the AOX family of enzymes, HYD (Supplemental Figure S7) [62, 63]. Compared to unsynchronized animals, significant differences in the number of STRA8-positive spermatogonia per average number of Sertoli cells were detected in animals maintained on the WIN7D + RA + 8D, WIN7D + RA + HYD8D, and WIN7D + RA + WIN/HYD8D treatment schemes (Figure 5F; n = 3). No significant differences in the number of STRA8-positive spermatogonia per average number of Sertoli cells were detected in the WIN7D + RA + WIN8D treatment group (Figure 5F; n = 3). A significant increase in the number of ZBTB16-positive spermatogonia was detected in all treatment groups compared to the unsynchronized animals (Figure 5E; n = 3).

Concurrent maintenance on WIN/HYD for one spermatogenic cycle following the WIN7D + RA synchrony protocol increases the number of testis tubules missing germ cells expressing germ cell nuclear antigen

Our histological observations of the WIN7D + RA + WIN/HYD8D treated animals prompted us to quantify the number of testis tubules missing germ cells. Testis sections from WIN7D + RA + 8D, WIN7D + RA + WIN8D, WIN7D + RA + HYD8D, and WIN7D + RA + WIN/HYD8D treated animals were immunostained for the germ cell-specific marker GCNA (Figure 6A–D) [57]. Quantification revealed that 2% of the testis tubules within the WIN7D + RA + 8D, WIN7D + RA + HYD8D, and WIN7D + RA + WIN8D treated groups were missing cells or layers of GCNA-positive cells (Figure 6E; n = 3–4). In contrast, 36% of WIN7D + RA + WIN/HYD8D treated animals had testis tubules missing cells or layers of GCNA-positive cells (Figure 6E; n = 3–4).

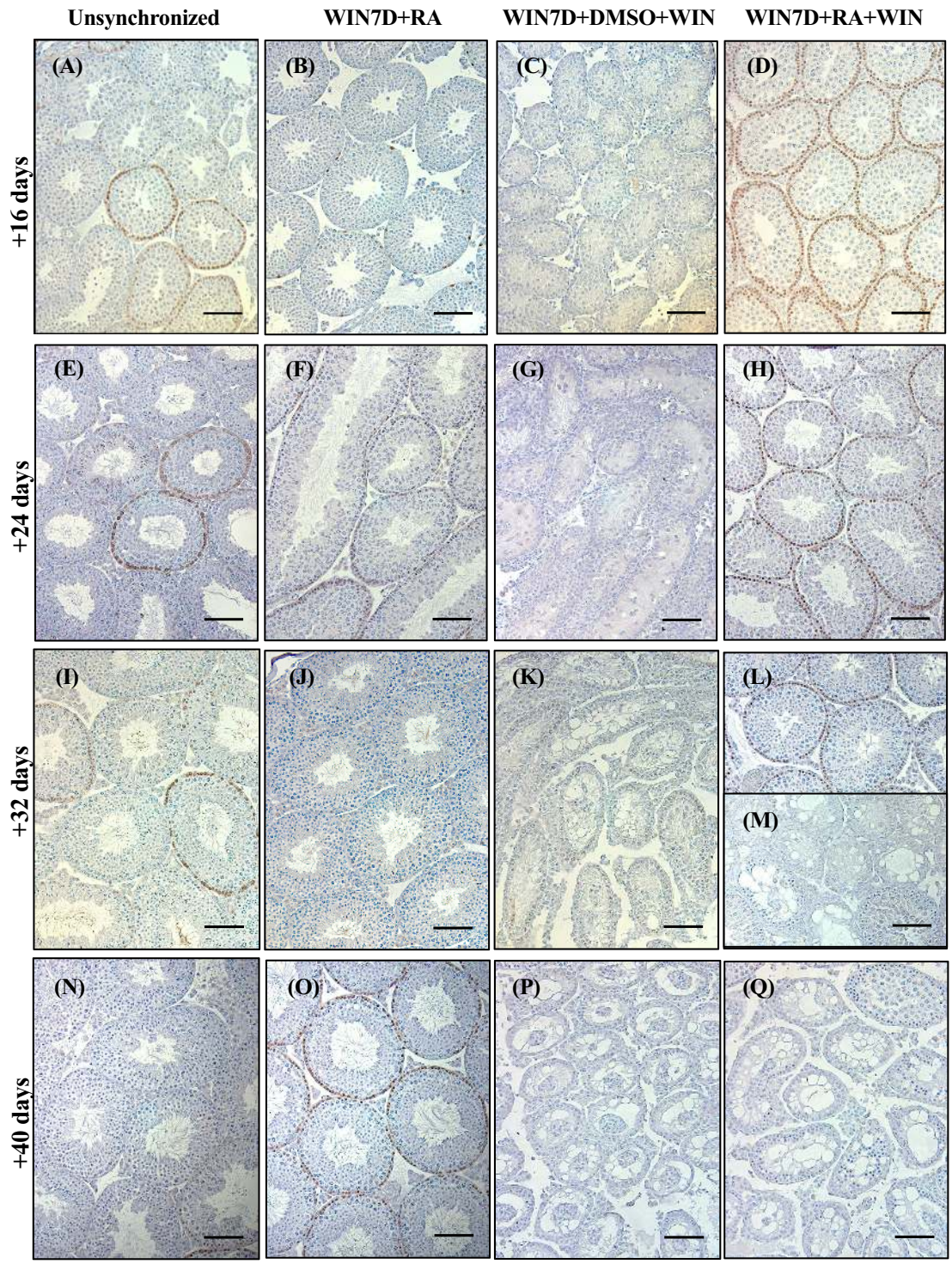

Figure 4. Maintenance on WIN for several spermatogenic cycles eventually results in degenerative seminiferous tubules. Immunostaining of testis sections from unsynchronized (**A**, **E, I,** and **N**), WIN7D + RA (**B**, **F, J,** and **O)**, WIN7D + DMSO + WIN (**C, G, K,** and **P**), and WIN7D + RA + WIN (**D**, **H**, **L, M,** and **Q**) treated mice for 16, 24, 32, and 40 additional maintenance days. Testis sections were immunostained for STRA8. Immunopositive cells are indicated by brown precipitate. Scale bar = 100 μM. n = 3–4.

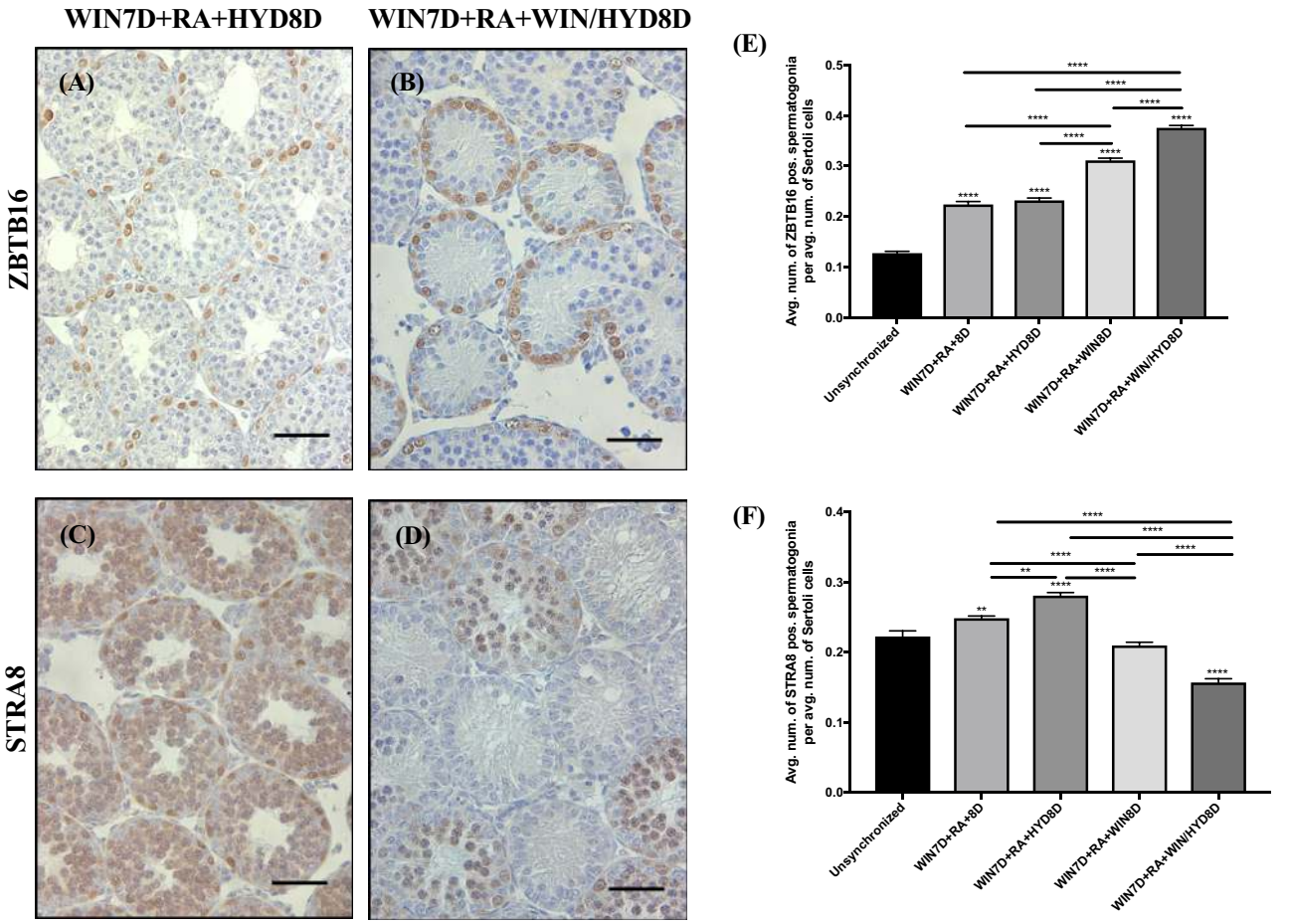

Figure 5. WIN7D + RA + HYD8D animals do not show any spermatogenic defects, although WIN7D + RA + WIN/HYD8D animals show an increased number of ZBTB16-positive spermatogonia. Immunostaining of testis sections for ZBTB16 and STRA8 for WIN7D + RA + HYD8D (**A** and **B**) and WIN7D + RA + WIN/HYD8D treated mice (**C** and **D**). Graphical representation of the average number of ZBTB16- (**E**) and STRA8-positive (**F**) spermatogonia per tubule within each treatment group. Asterisks represent statistical difference of a treatment group compared to control. Black lines indicate statistical significance between treatment groups. Animals were 17 dpp at euthanasia. Scale bar = 100 μM. n = 3. $^{*}P < 0.05$, $^{**}P < 0.01$, $^{****}P < 0.0001$.

Discussion

It is well established that *at*RA is absolutely required for spermatogonial differentiation [9, 11]; however, many gaps still remain in our understanding of the enzymatic and cellular sources responsible for generating *at*RA. Using a genetic model, Raverdeau and colleagues demonstrated that *at*RA in the first round of spermatogenesis is synthesized by the ALDH1A enzymes within Sertoli cells [31]. Importantly, if the mice with all three ALDH1A enzymes deleted in Sertoli cells were given a single injection of *at*RA, spermatogenesis resumed and was maintained suggesting that the *at*RA injection resulted in an alternate source of continuous *at*RA synthesis [31]. However, the cellular and enzymatic source(s) of *at*RA driving these subsequent rounds of spermatogonial differentiation is a key research question that remains to be fully addressed.

ALDH1A2 is a cytoplasmic *at*RA-generating enzyme enriched in meiotic and postmeiotic germ cells within the murine testis [24, 64, 65]. Previous publications have provided evidence to suggest that this enzyme may be the primary source of *at*RA synthesis driving subsequent rounds of spermatogenesis. However, our present findings do not support a role for ALDH1A2 as an essential enzyme to testicular *at*RA biosynthesis, as severe deficiency of *Aldh1a2* within the postnatal testis in either the germ cell cKO or the *Aldh1a2*$^{\Delta/\Delta}$, CreER^{T2} animals analyzed in this study did not result in significantly reduced *at*RA levels. Interestingly, *Cyp26a1* has been suggested to be a reliable indicator of endogenous *at*RA levels, yet the significant reduction in *Cyp26a1* expression in both the germ cell cKO and the *Aldh1a2*$^{\Delta/\Delta}$, CreER^{T2} animals was not reflective of endogenous levels of total testicular *at*RA. The biological function of the CYP26 enzymes is to metabolize *at*RA into inactive metabolites [20, 66–68]. Therefore, the reduction in *Cyp26a1* expression may actually be suggestive of a feedback mechanism that is lowering degradation activities in order to sustain higher levels *at*RA within the *Aldh1a2* cKO and *Aldh1a2*$^{\Delta/\Delta}$, CreER^{T2} testes. It is also possible that the reduction in *Cyp26a1* may allow for circulating extratesticular *at*RA to enter the testis, although this possibility seems unlikely as it has recently been reported that CYP26B1, not CYP26A1, is the major isomer involved in the regulation of *at*RA levels within the seminiferous epithelium [55]. Therefore, future investigations using radiolabeled *at*RA within these *Aldh1a2* cKO testes are required to further investigate this possibility.

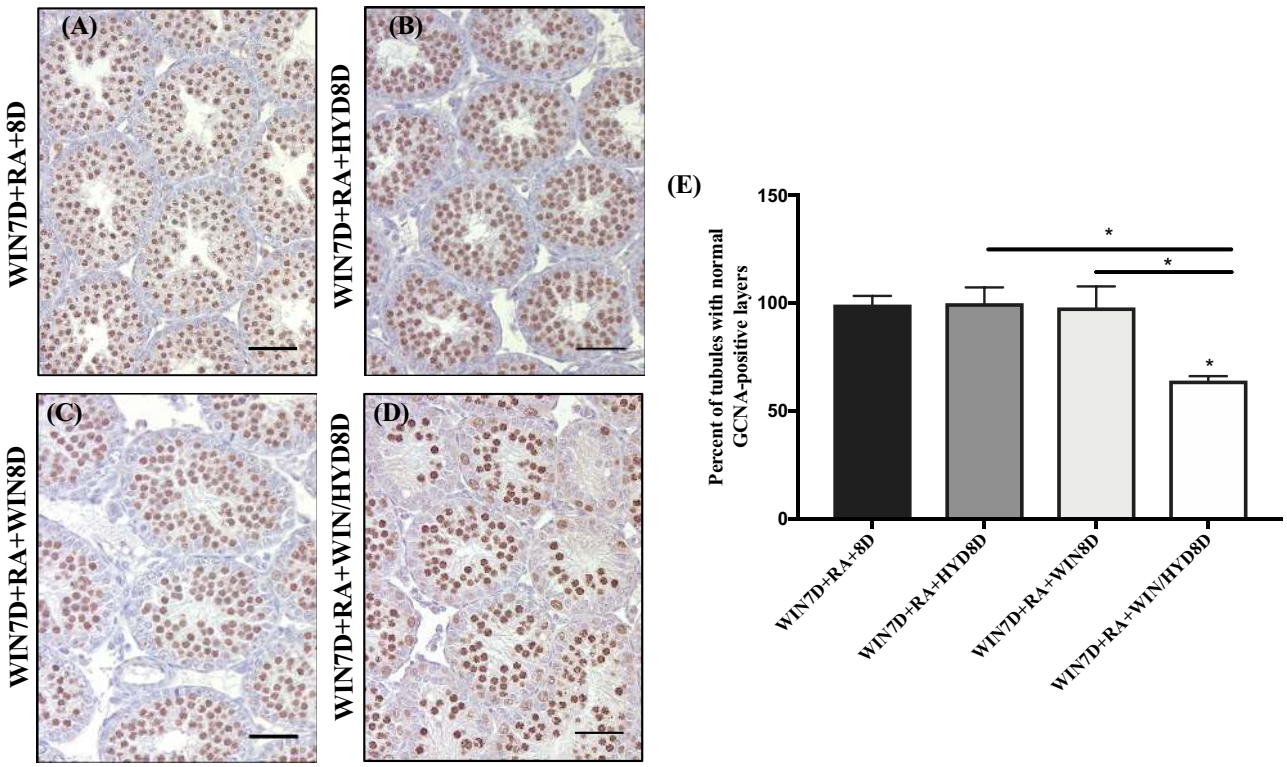

Figure 6. WIN7D + RA + WIN/HYD8D animals have an increased number of tubules with abnormal or missing layers of GCNA-positive germ cells. Representative testis sections from WIN7D + RA + 8D (**A**), WIN7D + RA + HYD8D (**B**), WIN7D + RA + WIN8D (**C**), and WIN7D + RA + WIN/HYD8D (**D**) treated animals immunostained for GCNA. Immunopositive cells are indicated by brown precipitate. (**E**) Graphical representation of the number of tubules from WIN7D + RA + 8D, WIN7D + RA + HYD8D, WIN7D + RA + WIN8D, and WIN7D + RA + WIN/HYD8D treated testes containing normal GCNA-positive germ cell layers. Asterisks represent statistical difference of a treatment group compared to control. Black lines represent statistical significance between treatment groups. Animals were 17 dpp at euthanasia. n = 3–4. $^{*}P < 0.05$.

It has been widely hypothesized that the *at*RA required for spermatogenesis is made inside the epithelium [35]. In support of this hypothesis, Kurlandsky and colleagues found that less than 1% of circulating *at*RA enters the seminiferous epithelium [69], which is not enough to elicit the responses that we observed. Therefore, we hypothesized that the levels of *at*RA detected within the *Aldh1a2* germ cell cKO and *Aldh1a2*$^{\Delta/\Delta}$, CreER^{T2} testes could be due to compensation by the other ALDH1A enzymes (*Aldh1a1* and *Aldh1a3*). We tested this hypothesis pharmacologically by inhibiting the activities of the ALDH1A enzymes using the pan-ALDH1A inhibitor WIN 18446. In the absence of an *at*RA pulse or injection, the ZBTB16-positive spermatogonia accumulated but no differentiated STRA8-positive spermatogonia appeared. If given a single injection of *at*RA, our analysis revealed that the ZBTB16-positive population was sensitive to continued maintenance on WIN; however, we observed no significant reductions in the number of STRA8-positive spermatogonia or *at*RA levels. Further, we found that approximately 32–40 days of continuous WIN treatment was required to induce a severe degenerative phenotype if a single *at*RA pulse was given at 9 dpp. It is presently unclear why treatment with WIN requires such a prolonged period of time before cessation of spermatogenesis occurs. However, our data demonstrate that once the testis receives an *at*RA pulse, produced in situ by Sertoli cells or by injection, potent inhibition of the ALDH1A enzymes is insufficient to immediately inhibit subsequent rounds of spermatogonial differentiation.

Although the ALDH1A enzymes are the only family of enzymes currently implicated in the oxidation of *at*RAL to *at*RA in the mammalian testis, multiple enzyme families are able to perform this same metabolic step in other retinoid-dependent organs, such as the liver [43, 70–72]. The AOX enzymes are of particular interest as transcripts for two of the AOX isomers were significantly upregulated in testis microarray studies previously performed in our laboratory. *Aox4* was upregulated in germ cells compared to Sertoli cells during a synchronized first round of spermatogenesis [60]. *Aox3* was significantly upregulated in another microarray study aimed at identifying transcripts differentially expressed in spermatogenic stages in the adult testis, with maximal expression observed in stages VI–VIII [61]. *Aox3* mRNA has also been detected in germ cells via in situ hybridization [73]. However, the K_m values for the AOX enzymes is a magnitude higher than those reported for the ALDH1A enzymes, and because of this the AOX enzymes may only play a physiologically relevant role in testicular *at*RA biosynthesis when the ALDH1A enzymes are inactive [74–76]. Accordingly, the *Aox4*-null mouse is fully fertile, supporting a secondary role for these enzymes in testicular *at*RA biosynthesis [72]. Presently, very little is known about the role of AOX3 within the postnatal testis, as no genetic knockout models have been produced to date. Future studies of the *Aox3*-null mouse and ALDH1A/AOX compound animals will further elucidate the role that these enzymes play in testicular *at*RA biosynthesis.

We found the WIN7D + DMSO + WIN animals particularly interesting, as histological analysis of these animals demonstrated that the dosage of WIN utilized in our studies was sufficient to block spermatogonial differentiation for prolonged periods of time. Surprisingly, *at*RA measurements revealed residual levels of *at*RA

remaining in the WIN7D + DMSO + WIN8D treated testes. This was consistent with other studies, in which residual amounts of *at*RA were detected even though histological analysis confirmed that WIN treatment resulted in the complete loss of advanced germ cells and cessation of spermatogenesis [37, 77, 78]. These findings lead us to hypothesize that the A to A1 transition may require a certain threshold of *at*RA that can only be met when the ALDH1A enzymes are fully functional.

The requirement for *at*RA in spermatogonial differentiation, meiotic initiation, blood–testis barrier formation, spermiogenesis, and spermiation has been well studied. However, investigations of how and where *at*RA is produced to drive these processes have been complicated by gaps in our knowledge of the enzymes responsible for *at*RA biosynthesis. Although the expression of ALDH1A1 residing within adult Sertoli cells may contribute to the biosynthesis of *at*RA driving the premeiotic transitions, several groups have provided evidence to suggest that ALDH1A2 residing within the meiotic and postmeiotic germ cells is the major isomer involved [31, 32, 38, 45]. In this report, we have examined for the first time the in vivo contribution of ALDH1A2 to postnatal testicular *at*RA levels using two complementary genetic approaches. Our results demonstrate that severe deficiency of *Aldh1a2* did not result in any adverse effects on male fertility or health. This report also provides evidence suggesting that the AOX family of enzymes may play a physiologically relevant role in testicular *at*RA biosynthesis, specifically following an injection of *at*RA when the ALDH1A enzymes are inhibited.

Supplementary data

Supplementary data are available at *BIOLRE* online.

Supplemental Figure S1. Generation of conditional allele to knock out the *Aldh1a2* gene. The conditional allele for *Aldh1a2* was generated via a sequence replacement strategy. The diagram shows the wild-type *Aldh1a2* allele (top row), targeting construct (second row), homologous recombinant (third row), targeted conditional *Aldh1a2* allele without the neo cassette (fourth row), and the *Cre*-mediated deletion of the *Aldh1a2* gene (fifth row). The targeting construct contained (1) loxP sites that flanked exon 4, (2) a 2.5 kb 5′ short arm of homology, (3) a 5.6 kb 3′ long arm of homology, (4) a Diphtheria Toxin A (DTA) cassette, and (6) a Neomycin (Neo) cassette flanked by FRT sites for selective deletion. The Neo element allowed for positive selection in ES cells, while the DTA element allowed for negative selection in ES cells. After homologous recombination of the conditional knockout construct, the *Aldh1a2* gene will have normal expression until *Cre*-mediated deletion of exon 4. Deletion of exon 4 creates a frameshift mutation and a premature stop, which renders the *Aldh1a2* gene inactive.

Supplemental Figure S2. Schematic of the WIN maintenance regimens. Control animals were fed 1% gum tragacanth for the entirety of the treatment regimen. Two dpp male mice were given 100 mg/kg WIN daily for seven consecutive days, given an *at*RA injection at 9 dpp and then maintained on 1% gum tragacanth (WIN7D + RA), 150 mg/kg WIN (WIN7D + RA + WIN), 25 mg/kg HYD (WIN7D + RA + HYD) or 150 mg/kg WIN and 25 mg/kg HYD (WIN7D + RA + WIN/HYD). Another group of animals were also fed 100 mg/kg WIN from 2–8 dpp, followed by a DMSO injection at 9 dpp and maintained on 150 mg/kg WIN (WIN7D + DMSO + WIN). Depending on the experiment, maintenance animals were maintained on their treatment schemes for 8, 16, 24, 32, or 40 days.

Supplemental Figure S3. Elimination of *Aldh1a2* using the *Stra8*-Cre. Control (*Aldh1a2*$^{fl/fl}$, *Stra8*-Cre–) and cKO (*Aldh1a2*$^{fl/fl}$, *Stra8*-Cre+) animals analyzed at 60 dpp. Representative cross-sections for control (**A, B**) and cKO (**C, D**) animals, stained for ALDH1A2. Immunopositive cells are indicated by brown precipitate. (**E**) qRT-PCR analysis of *Aldh1a2, Aldh1a1, Aldh1a3, Stra8,* and *Cyp26a1*. (**F**) Graphical representation of *at*RA measurements. Scale bars = 100 μM. for n = 3–6. $^{*}P < 0.05$, and $^{**}P < 0.01$.

Supplemental Figure S4. Body weight in tamoxifen injected *Aldh1a2*, CreER^{T2} animals. Body weight of *Aldh1a2*$^{+/+}$, CreER^{T2}; *Aldh1a2*$^{+/Ä}$, CreER^{T2}; and *Aldh1a2*$^{Ä/Ä}$, CreER^{T2} animals injected with tamoxifen at 8 and 21 dpp. Body weights were measured in grams (g) on the day of euthanasia, n = 5–8.

Supplemental Figure S5. WIN maintenance regimen, changes in body weight, and average testis weight. (**A**) Schematic of the WIN maintenance regimen across one spermatogenic cycle. (**B**) Average body weight measured in grams (g) over the 8-day maintenance regimen (n = 28–46). (**C**) Average testis weight measured in grams (g) on the day of euthanasia (n = 8–46). Asterisks represent statistical difference of a treatment group compared to control. Black lines represent statistical significance between treatment groups. $^{****}P < 0.0001$.

Supplemental Figure S6. Schematic of the WIN maintenance regimen across several spermatogenic cycles. Unsynchronized animals were fed 1% gum tragacanth for 16, 24, 32, or 40 days. Two dpp male mice were given 100 mg/kg WIN daily for seven consecutive days and then placed in one of the following three treatment groups: (1) *at*RA injection at 9 dpp and maintained on 1% gum tragacanth for 16, 24, 32, or 40 days (WIN7D + RA); (2) *at*RA injection at 9 dpp and maintained on 150 mg/kg WIN for 16, 24, 32, or 40 days (WIN7D + RA + WIN); or (3) DMSO injection at 9 dpp and maintained on 150 mg/kg WIN for 16, 24, 32, or 40 days (WIN7D + DMSO + WIN).

Supplemental Figure S7. Schematic of the treatment regimen for animals maintained solely on HYD or concurrently on WIN and HYD following the WIN + RA synchrony protocol. Two dpp male mice were given 100 mg/kg WIN daily for seven consecutive days, injected with *at*RA at 9 dpp and maintained either on 25 mg/kg HYD (WIN7D + RA + HYD8D) or maintained concurrently on 150 mg/kg WIN and 25 mg/kg HYD for 8 additional days (WIN7D + RA + WIN/HYD8D).

Supplemental Table S1. PCR primers for genotyping.

Supplemental Table S2. Primers for quantitative RT-PCR.

Supplemental Table S3. Male fertility data for Aldhla2fl/fl, Stra8-Cre mutant mice.

Acknowledgments

We are most grateful to Dr Joseph L. Napoli for the donation of the *Aldh1a2*$^{fl/fl}$ transgenic line as well as the technical support provided by the Mouse Biology Program (MBP) at the University of California, Davis. We would like to thank Dr John Amory for the kind gift of the WIN 18,446 compound. We would also like to acknowledge Rachel Gewiss, Debra Mitchell, Zane Rivers, and Quinton Beedle for their technical assistance, helpful comments, and critical reading of the manuscript.

References

1. Yang QE, Oatley JM. Spermatogonial stem cell functions in physiological and pathological conditions. *Curr Top Dev Biol* 2014; **107**: 235–267.
2. Busada JT, Geyer CB. The role of retinoic acid (RA) in spermatogonial differentiation. *Biol Reprod* 2016; **94**:10.

3. Drumond AL, Meistrich ML, Chiarini-Garcia H. Spermatogonial morphology and kinetics during testis development in mice: a high-resolution light microscopy approach. *Reproduction* 2011; **142**: 145–155.
4. Niedenberger BA, Busada JT, Geyer CB. Marker expression reveals heterogeneity of spermatogonia in the neonatal mouse testis. *Reproduction* 2015; **149**:329–338.
5. Oakberg EF. A description of spermiogenesis in the mouse and its use in analysis of the cycle of the seminiferous epithelium and germ cell renewal. *Am J Anat* 1956; **99**:391–413.
6. Russell L, Ettlin R, Sinha HA, Clegg E. *Histological and Histopathological Evaluation of the Testis Clearwater*. Florida: Cache River Press 1990.
7. Clermont Y, Trott M. Duration of the cycle of the seminiferous epithelium in the mouse and hamster determined by means of 3H-thymidine and radioautography. *Fertil Steril* 1969; **20**:805–817.
8. Hogarth C, Griswold M. Driving asynchronous spermatogenenesis: is retinoic acid the answer. *Anim Reprod* 2012; **9**:742–750.
9. Wolbach SB, Howe PR. Tissue changes following deprivation of fat-soluble a vitamin. *J Exp Med* 1925; **42**:753–777.
10. van Pelt AM, de Rooij DG. Retinoic acid is able to reinitiate spermatogenesis in vitamin A-deficient rats and high replicate doses support the full development of spermatogenic cells. *Endocrinology* 1991; **128**: 697–704.
11. Griswold MD, Bishop PD, Kim KH, Ping R, Siiteri JE, Morales C. Function of vitamin A in normal and synchronized seminiferous tubules. *Ann NY Acad Sci* 1989; **564**:154–172.
12. van Pelt AM, de Rooij DG. Synchronization of the seminiferous epithelium after vitamin A replacement in vitamin A-deficient mice. *Biol Reprod* 1990; **43**:363–367.
13. Duester G. Families of retinoid dehydrogenases regulating vitamin A function. *Eur J Biochem* 2000; **267**:4315–4324.
14. Pares X, Farres J, Kedishvili N, Duester G. Medium- and short-chain dehydrogenase/reductase gene and protein families. *Cell Mol Life Sci* 2008; **65**:3936–3949.
15. Boerman MH, Napoli JL. Effects of sulfhydryl reagents, retinoids, and solubilization on the activity of microsomal retinol dehydrogenase. *Arch Biochem Biophys* 1995; **321**:434–441.
16. Mertz JR, Shang E, Piantedosi R, Wei S, Wolgemuth DJ, Blaner WS. Identification and characterization of a stereospecific human enzyme that catalyzes 9-cis-retinol oxidation. *J Biol Chem* 1997; **272**:11744–11749.
17. Romert A, Tuvendal P, Simon A, Dencker L, Eriksson U. The identification of a 9-cis retinol dehydrogenase in the mouse embryo reveals a pathway for synthesis of 9-cis retinoic acid. *Proc Natl Acad Sci USA* 1998; **95**:4404–4409.
18. Lapshina EA, Belyaeva OV, Chumakova OV, Kedishvili NY. Differential recognition of the free versus bound retinol by human microsomal retinol/sterol dehydrogenases: characterization of the holo-CRBP dehydrogenase activity of RoDH-4. *Biochemistry* 2003; **42**:776–784.
19. Lee MO, Manthey CL, Sladek NE. Identification of mouse liver aldehyde dehydrogenases that catalyze the oxidation of retinaldehyde to retinoic acid. *Biochem Pharmacol* 1991; **42**:1279–1285.
20. Duester G. Retinoic acid synthesis and signaling during early organogenesis. *Cell* 2008; **134**:921–931.
21. Theodosiou M, Laudet V, Schubert M. From carrot to clinic: an overview of the retinoic acid signaling pathway. *Cell Mol Life Sci* 2010; **67**:1423–1445.
22. Niederreither K, McCaffery P, Drager UC, Chambon P, Dolle P. Restricted expression and retinoic acid-induced downregulation of the retinaldehyde dehydrogenase type 2 (RALDH-2) gene during mouse development. *Mech Dev* 1997; **62**:67–78.
23. Fan X, Molotkov A, Manabe S, Donmoyer CM, Deltour L, Foglio MH, Cuenca AE, Blaner WS, Lipton SA, Duester G. Targeted disruption of Aldh1a1 (Raldh1) provides evidence for a complex mechanism of retinoic acid synthesis in the developing retina. *Mol Cell Biol* 2003; **23**:4637–4648.
24. Wang X, Penzes P, Napoli JL. Cloning of a cDNA encoding an aldehyde dehydrogenase and its expression in *Escherichia coli*. *J Biol Chem* 1996; **271**:16288–16293.
25. Sima A, Parisotto M, Mader S, Bhat PV. Kinetic characterization of recombinant mouse retinal dehydrogenase types 3 and 4 for retinal substrates. *Biochim Biophys Acta* 2009; **1790**:1660–1664.
26. Grun F, Hirose Y, Kawauchi S, Ogura T, Umesono K. Aldehyde dehydrogenase 6, a cytosolic retinaldehyde dehydrogenase prominently expressed in sensory neuroepithelia during development. *J Biol Chem* 2000; **275**:41210–41218.
27. Vasiliou V, Pappa A, Estey T. Role of human aldehyde dehydrogenases in endobiotic and xenobiotic metabolism. *Drug Metab Rev* 2004; **36**:279–299.
28. Moretti A, Li J, Donini S, Sobol RW, Rizzi M, Garavaglia S. Crystal structure of human aldehyde dehydrogenase 1A3 complexed with NAD+ and retinoic acid. *Sci Rep* 2016; **6**:35710.
29. Moretti A, Li J, Donini S, Sobol WR, Garavaglia S. Crystal structure of human aldehyde dehydrogenase 1A3 complexed with NAD+ and retinoic acid. *Sci Rep* 2016; **6**.
30. Hsu LC, Chang WC, Yoshida A. Mouse type-2 retinaldehyde dehydrogenase (RALDH2): genomic organization, tissue-dependent expression, chromosome assignment and comparison to other types. *Biochim Biophys Acta* 2000; **1492**:289–293.
31. Raverdeau M, Gely-Pernot A, Feret B, Dennefeld C, Benoit G, Davidson I, Chambon P, Mark M, Ghyselinck NB. Retinoic acid induces Sertoli cell paracrine signals for spermatogonia differentiation but cell autonomously drives spermatocyte meiosis. *Proc Natl Acad Sci USA* 2012; **109**:16582–16587.
32. Endo T, Freinkman E, de Rooij DG, Page DC. Periodic production of retinoic acid by meiotic and somatic cells coordinates four transitions in mouse spermatogenesis. *Proc Natl Acad Sci USA* 2017; **114**:E10132–E10141.
33. Wu JW, Wang RY, Guo QS, Xu C. Expression of the retinoic acid-metabolizing enzymes RALDH2 and CYP26b1 during mouse postnatal testis development. *Asian J Androl* 2008; **10**:569–576.
34. Zhai Y, Sperkova Z, Napoli JL. Cellular expression of retinal dehydrogenase types 1 and 2: effects of vitamin A status on testis mRNA. *J Cell Physiol* 2001; **186**:220–232.
35. Vernet N, Dennefeld C, Rochette-Egly C, Oulad-Abdelghani M, Chambon P, Ghyselinck NB, Mark M. Retinoic acid metabolism and signaling pathways in the adult and developing mouse testis. *Endocrinology* 2006; **147**:96–110.
36. Arnold SL, Kent T, Hogarth CA, Schlatt S, Prasad B, Haenisch M, Walsh T, Muller CH, Griswold MD, Amory JK, Isoherranen N. Importance of ALDH1A enzymes in determining human testicular retinoic acid concentrations. *J Lipid Res* 2015; **56**:342–357.
37. Kent T, Arnold SL, Fasnacht R, Rowsey R, Mitchell D, Hogarth CA, Isoherranen N, Griswold MD. ALDH enzyme expression is independent of the spermatogenic cycle, and their inhibition causes misregulation of murine spermatogenic processes. *Biol Reprod* 2016; **94**:12.
38. Sugimoto R, Nabeshima Y, Yoshida S. Retinoic acid metabolism links the periodical differentiation of germ cells with the cycle of Sertoli cells in mouse seminiferous epithelium. *Mech Dev* 2012; **128**:610–624.
39. Niederreither K, Subbarayan V, Dolle P, Chambon P. Embryonic retinoic acid synthesis is essential for early mouse post-implantation development. *Nat Genet* 1999; **21**:444–448.
40. Mic FA, Haselbeck RJ, Cuenca AE, Duester G. Novel retinoic acid generating activities in the neural tube and heart identified by conditional rescue of Raldh2 null mutant mice. *Development* 2002; **129**:2271–2282.
41. Dupe V, Matt N, Garnier JM, Chambon P, Mark M, Ghyselinck NB. A newborn lethal defect due to inactivation of retinaldehyde dehydrogenase type 3 is prevented by maternal retinoic acid treatment. *Proc Natl Acad Sci USA* 2003; **100**:14036–14041.
42. Molotkova N, Molotkov A, Duester G. Role of retinoic acid during forebrain development begins late when Raldh3 generates retinoic acid in the ventral subventricular zone. *Dev Biol* 2007; **303**:601–610.
43. Arnold SL, Kent T, Hogarth CA, Griswold MD, Amory JK, Isoherranen N. Pharmacological inhibition of ALDH1A in mice decreases all-trans retinoic acid concentrations in a tissue specific manner. *Biochem Pharmacol* 2015; **95**:177–192.

44. Hogarth CA, Evanoff R, Mitchell D, Kent T, Small C, Amory JK, Griswold MD. Turning a spermatogenic wave into a tsunami: synchronizing murine spermatogenesis using WIN 18,4461. *Biol Reprod* 2013; **88**:40.
45. Kasimanickam VR. Expression of retinoic acid-metabolizing enzymes, ALDH1A1, ALDH1A2, ALDH1A3, CYP26A1, CYP26B1 and CYP26C1 in canine testis during post-natal development. *Reprod Dom Anim* 2016; **51**:901–909.
46. Niederreither K, Vermot J, Le Roux I, Schuhbaur B, Chambon P, Dolle P. The regional pattern of retinoic acid synthesis by RALDH2 is essential for the development of posterior pharyngeal arches and the enteric nervous system. *Development* 2003; **130**:2525–2534.
47. Sadate-Ngatchou PI, Payne CJ, Dearth AT, Braun RE. Cre recombinase activity specific to postnatal, premeiotic male germ cells in transgenic mice. *Genesis* 2008; **46**:738–742.
48. Feil S, Valtcheva N, Feil R. Inducible Cre mice. *Methods Mol Biol* 2009; **530**:343–363.
49. Livak KJ, Schmittgen TD. Analysis of relative gene expression data using real-time quantitative PCR and the 2(-Delta Delta C(T)) Method. *Methods* 2001; **25**:402–408.
50. Hogarth C, Griswold M. Immunohistochemical approaches for the study of spermatogenesis. *Methods Mol Biol* 2013; **927**:309–320.
51. Hogarth CA, Arnold S, Kent T, Mitchell D, Isoherranen N, Griswold MD. Processive pulses of retinoic acid propel asynchronous and continuous murine sperm production. *Biol Reprod* 2015; **92**:37.
52. Arnold SL, Amory JK, Walsh TJ, Isoherranen N. A sensitive and specific method for measurement of multiple retinoids in human serum with UHPLC-MS/MS. *J Lipid Res* 2012; **53**:587–598.
53. Stevison F, Hogarth C, Tripathy S, Kent T, Isoherranen N. Inhibition of the all-trans retinoic acid (at RA) hydroxylases CYP26A1 and CYP26B1 results in dynamic, tissue-specific changes in endogenous at RA signaling. *Drug Metab Dispos* 2017; **45**:846–854.
54. Hogarth CA, Evanoff R, Snyder E, Kent T, Mitchell D, Small C, Amory JK, Griswold MD. Suppression of Stra8 expression in the mouse gonad by WIN 18,4461. *Biol Reprod* 2011; **84**:957–965.
55. Ross AC. Retinoid production and catabolism: role of diet in regulating retinol esterification and retinoic acid oxidation. *J Nutr* 2003; **133**:291S–296S.
56. DeFalco T, Potter SJ, Williams AV, Waller B, Kan MJ, Capel B. Macrophages contribute to the spermatogonial niche in the adult testis. *Cell Rep* 2015; **12**:1107–1119.
57. Buaas FW, Kirsh AL, Sharma M, McLean DJ, Morris JL, Griswold MD, de Rooij DG, Braun RE. Plzf is required in adult male germ cells for stem cell self-renewal. *Nat Genet* 2004; **36**:647–652.
58. Costoya JA, Hobbs RM, Barna M, Cattoretti G, Manova K, Sukhwani M, Orwig KE, Wolgemuth DJ, Pandolfi PP. Essential role of Plzf in maintenance of spermatogonial stem cells. *Nat Genet* 2004; **36**:653–659.
59. Zhou Q, Li Y, Nie R, Friel P, Mitchell D, Evanoff RM, Pouchnik D, Banasik B, McCarrey JR, Small C, Griswold MD. Expression of stimulated by retinoic acid gene 8 (Stra8) and maturation of murine gonocytes and spermatogonia induced by retinoic acid in vitro. *Biol Reprod* 2008; **78**:537–545.
60. Evans E, Hogarth C, Mitchell D, Griswold M. Riding the spermatogenic wave: profiling gene expression within neonatal germ and sertoli cells during a synchronized initial wave of spermatogenesis in mice. *Biol Reprod* 2014; **90**:108.
61. Jauregui EJ, Mitchell D, Garza SM, Topping T, Hogarth CA, Griswold MD. Leydig cell genes change their expression and association with polysomes in a stage-specific manner in the adult mouse testis. *Biol Reprod* 2018; **98**:722–738.
62. Strelevitz TJ, Orozco CC, Obach RS. Hydralazine as a selective probe inactivator of aldehyde oxidase in human hepatocytes: estimation of the contribution of aldehyde oxidase to metabolic clearance. *Drug Metab Dispos* 2012; **40**:1441–1448.
63. Johnson C, Stubley-Beedham C, Stell JG. Hydralazine: a potent inhibitor of aldehyde oxidase activity in vitro and in vivo. *Biochem Pharmacol* 1985; **34**:4251–4256.
64. Nishimura M, Naito S. Tissue-specific mRNA expression profiles of human phase I metabolizing enzymes except for cytochrome P450 and phase II metabolizing enzymes. *Drug Metab Pharmacokinet* 2006; **21**:357–374.
65. Alnouti Y, Klaassen CD. Tissue distribution, ontogeny, and regulation of aldehyde dehydrogenase (Aldh) enzymes mRNA by prototypical microsomal enzyme inducers in mice. *Toxicol Sci* 2008; **101**:51–64.
66. Thatcher JE, Isoherranen N. The role of CYP26 enzymes in retinoic acid clearance. *Expert Opin Drug Metab Toxicol* 2009; **5**:875–886.
67. Kedishvili NY. Enzymology of retinoic acid biosynthesis and degradation. *J Lipid Res* 2013; **54**:1744–1760.
68. Fiorella PD, Napoli JL. Microsomal retinoic acid metabolism. Effects of cellular retinoic acid-binding protein (type I) and C18-hydroxylation as an initial step. *J Biol Chem* 1994; **269**:10538–10544.
69. Kurlandsky SB, Gamble MV, Ramakrishnan R, Blaner WS. Plasma delivery of retinoic acid to tissues in the rat. *J Biol Chem* 1995; **270**:17850–17857.
70. Vila R, Kurosaki M, Barzago MM, Kolek M, Bastone A, Colombo L, Salmona M, Terao M, Garattini E. Regulation and biochemistry of mouse molybdo-flavoenzymes. The DBA/2 mouse is selectively deficient in the expression of aldehyde oxidase homologues 1 and 2 and represents a unique source for the purification and characterization of aldehyde oxidase. *J Biol Chem* 2004; **279**:8668–8683.
71. Huang DY, Furukawa A, Ichikawa Y. Molecular cloning of retinal oxidase/aldehyde oxidase cDNAs from rabbit and mouse livers and functional expression of recombinant mouse retinal oxidase cDNA in *Escherichia coli*. *Arch Biochem Biophys* 1999; **364**:264–272.
72. Terao M, Kurosaki M, Marini M, Vanoni MA, Saltini G, Bonetto V, Bastone A, Federico C, Saccone S, Fanelli R, Salmona M, Garattini E. Purification of the aldehyde oxidase homolog 1 (AOH1) protein and cloning of the AOH1 and aldehyde oxidase homolog 2 (AOH2) genes. Identification of a novel molybdo-flavoprotein gene cluster on mouse chromosome 1. *J Biol Chem* 2001; **276**:46347–46363.
73. Terao M, Kurosaki M, Saltini G, Demontis S, Marini M, Salmona M, Garattini E. Cloning of the cDNAs coding for two novel molybdo-flavoproteins showing high similarity with aldehyde oxidase and xanthine oxidoreductase. *J Biol Chem* 2000; **275**:30690–30700.
74. Garattini E, Fratelli M, Terao M. The mammalian aldehyde oxidase gene family. *Hum Genomics* 2009; **4**:119–130.
75. Chen Y, Koppaka V, Thompson DC, Vasiliou V. Focus on molecules: ALDH1A1: from lens and corneal crystallin to stem cell marker. *Exp Eye Res* 2012; **102**:105–106.
76. Yoshida A, Hsu LC, Dave V. Retinal oxidation activity and biological role of human cytosolic aldehyde dehydrogenase. *Enzyme* 1992; **46**:239–244.
77. Paik J, Haenisch M, Muller CH, Goldstein AS, Arnold S, Isoherranen N, Brabb T, Treuting PM, Amory JK. Inhibition of retinoic acid biosynthesis by the bisdichloroacetyldiamine WIN 18,446 markedly suppresses spermatogenesis and alters retinoid metabolism in mice. *J Biol Chem* 2014; **289**:15104–15117.
78. Amory JK, Muller CH, Shimshoni JA, Isoherranen N, Paik J, Moreb JS, Amory DW, Sr, Evanoff R, Goldstein AS, Griswold MD. Suppression of spermatogenesis by bisdichloroacetyldiamines is mediated by inhibition of testicular retinoic acid biosynthesis. *J Androl* 2011; **32**:111–119.